

USING AIRBORNE MULTISPECTRAL IMAGERY TO MONITOR COTTON ROOT ROT EXPANSION WITHIN A GROWING SEASON

Chenghai Yang

USDA-ARS

Weslaco, TX

Gary N. Odvody

Carlos J. Fernandez

Juan A. Landivar

Texas AgriLife Research and Extension Center

Corpus Christi, TX

Richard R. Minzenmayer

Texas AgriLife Extension, Ballinger, TX

Robert L. Nichols

Cotton Incorporated

Cary, NC

Abstract

Cotton root rot is a serious and destructive disease that affects cotton production in the southwestern United States. Accurate delineation of cotton root rot infestations is important for cost-effective management of the disease. The objective of this study was to use airborne multispectral imagery for detecting and monitoring the expansion of root rot infestations within cotton fields during a growing season. A number of cotton fields near Edroy and San Angelo, Texas were selected for this study. Airborne multispectral digital imagery with blue, green, red and near-infrared bands was taken from these fields 2-4 times during the 2010 growing season. The imagery for two fields from each of the two locations was georeferenced, classified into 2-12 spectral classes using unsupervised classification techniques, and then grouped into root rot-infested and non-infested zones. The infested areas within each field were determined for each imaging date and compared among the different dates. Both airborne imagery and ground observations showed that cotton root rot expanded in different patterns and at different rates over the growing season. Towards the end of the growing season, the percentage of root rot-infested areas increased to 13.6% and 21.6% in the two fields in Edroy, and to 40.4% and 52.3% in the two fields in San Angelo. The results from this study will be useful for the understanding of the progression of the disease and for the development of site-specific treatment plans for the disease.

Introduction

Cotton root rot, caused by the fungus *Phymatotrichopsis omnivora*, is one of the most destructive plant diseases and occurs throughout the southwestern United States. It has an extremely wide host range and has been reported as a pathogen of over 2000 dicotyledonous plants (Olsen, 2009). Cotton (*Gossypium hirsutum* L.) is an economically important crop that is highly susceptible to this disease. Infected plants wilt and quickly die in several days with the leaves attached to the plants. The fungus kills plants typically in circular areas ranging from less than a square meter to several hectares in size (Smith et al., 1962). The symptoms usually begin during the period of rapid vegetative growth, are more visible during flowering and fruit development, and continue to increase through the growing season. The disease tends to occur in the same areas of the field in recurring years, but varies in intensity from year to year. It usually spreads more during rainy years as moisture favors all aspects of the disease cycle. Plants infected earlier in the growing season will die before bearing fruit, whereas infection occurring at later plant growth stages will reduce cotton yield and lower lint quality (Ezekiel and Taubenhaus, 1934; Yang et al., 2005).

Cotton root rot has plagued the cotton industry for more than 100 years. Despite decades of research efforts, effective practices for control of this disease are still lacking. Cultural practices such as deep ploughing, organic amendments, late planting, and rotation with monocotyledonous crops have been used to reduce the occurrence and severity of the disease (Smith et al., 1962; Rush and Lyda, 1984; Fernandez, 2005). Some fumigants and fungicides applied to root rot-infested areas have shown reductions in the incidence of the disease, but they are not always effective and economical for long-term control (Lyda et al., 1967; Lyda and Burnett, 1970; Whitson and Hine, 1986; Rush and Lyda, 1989). More recently, new fungicides were evaluated and a commercial formulation of flutriafol (TOPGUARD® - Cheminova, Inc., Wayne, NJ) applied via drip irrigation was found to effectively control cotton root rot (Isakeit et al., 2007, 2009). More experiments are being conducted to determine effective rates, application

methods and timing on the use of this fungicide for both irrigated and dryland cotton fields. Because of the cost concern, it is not appropriate to treat the whole field if only portions of the field are infected. Therefore, it is necessary to define the infested areas and understand the seasonal spread of the disease within fields so that variable rate technology can be used to apply the fungicide only to the infested areas for more effective and economical control.

Remote sensing is perhaps the only practical means for effectively mapping this disease because of large numbers of infested areas and their irregular shapes within cotton fields. In fact, this technology has long been used to document the distributions of cotton root rot damage with cotton fields (Taubenhaus et al., 1929; Nixon et al., 1975; 1987). More recently, Yang et al. (2005) integrated airborne multispectral digital imagery with global positioning system (GPS) and image classification techniques to accurately detect and map root rot infestations within cotton fields in south Texas for site-specific management. Yang et al. (2010) compared airborne multispectral and hyperspectral imagery for detecting and mapping root rot areas in cotton fields. Image classification and accuracy assessment of the root rot maps showed that both types of imagery accurately identified root rot-infested areas. These results indicate that either airborne multispectral or hyperspectral imagery can be used for assessing root rot infestations within cotton fields.

In previous studies, remote sensing imagery has been successfully used to map cotton root rot infestations near the end of the growing season when cotton root rot is fully pronounced for the season. However, little work has been done to monitor the progression of the disease over the growing season. This information is important for the understanding of the initiation and subsequent development and expansion of the disease. It can also be used to formulate the site-specific strategies for within-season control of the disease. Therefore, the objective of this study was to use airborne multispectral imagery for detecting and monitoring the progression of cotton root rot infestations in cotton fields within a growing season.

Materials and Methods

Study Sites

This study was conducted at two cotton growing areas in Texas, one in Edroy and one in San Angelo. Approximately a dozen irrigated and dryland fields were selected from each area for aerial imaging, but two representative fields from each area were used in this article. These fields had a history of cotton root rot. Table 1 shows the geographical locations and irrigation type for the fields at the two study sites.

Table 1. Geographical locations and irrigation type for the cotton fields at the two study sites.

Edroy Area				San Angelo Area			
Field	Latitude	Longitude	Irrigation type	Field	Latitude	Longitude	Irrigation type
1	28°07'38.8" N	97°41'43.8" W	Center pivot	1	31°26'30.7" N	100°22'16.1" W	Drip
2	27°59'53.3" N	97°42'48.5" W	Dryland	2	31°24'12.3" N	100°08'21.5" W	Center pivot

Airborne Multispectral Image Acquisition

Airborne multispectral imagery was acquired using a four-band imaging system described by Yang (2010). The system consists of four high resolution charge-coupled device (CCD) digital cameras and a ruggedized PC equipped with a frame grabber and image acquisition software. The cameras are sensitive in the 400 to 1000 nm spectral range and provide 2048 × 2048 active pixels with 12-bit data depth. A 24 mm lens is attached to each camera, resulting in an imaging size of 0.63 times the flight altitude. The four cameras are equipped with blue (430-470 nm), green (530-570 nm), red (630-670 nm), and near-infrared (NIR) (810-850 nm) bandpass interference filters, respectively. They are arranged in a quad configuration and attached to adjustable mounts that facilitate aligning the cameras horizontally, vertically, and rotationally. The image acquisition software allows the synchronized black-and-white band images from the cameras to be viewed on the computer monitor in any one of the four modes: a quad, one band image at a time, a normal color composite, or a color-infrared (CIR) composite. The band images are refreshed continuously to allow the operator to selectively save images with correct areas of interest. The selected four-band composite image is saved as a tiff file and consecutive images can be saved at 1-s intervals.

A Cessna 206 single-engine aircraft and a Cessna 404 twin-engine aircraft were used to acquire imagery from field 1 on four dates (12, 30 July, 11 and 23 August) and from field 2 on two dates (12 and 30 July) in the Edroy area, and from both fields in the San Angelo area on three dates (25 July, 23 August, and 27 September) during the 2010 growing season. All images were acquired at altitudes of 2440-2740 (8000-9000 ft) between 1130h and 1430h local time under sunny conditions. The ground pixel size achieved was 0.75-0.85 m.

Image Alignment and Rectification

An image-to-image registration procedure based on the first-order polynomial transformation model was used to align the four individual band images in each composite image. The red band image was used as the reference and the other three band images in each composite were registered to it to correct the misalignments among the four band images. One different transformation model was required for each of the three bands. To determine the transformation model coefficients, 8-12 evenly-distributed reference points were identified from each image. The root mean square (RMS) errors among the bands were generally from half a pixel to less than 2 pixels for the images.

The registered images were then georeferenced or rectified to the Universal Transverse Mercator (UTM), World Geodetic Survey 1984 (WGS-84), Zone 14, coordinate system based on a set of ground control points (12-15) around each field located with a Trimble GPS Pathfinder ProXRT receiver (Trimble Navigation Limited, Sunnyvale, California). The OmniSTAR XP satellite-based differential correction service (OmniSTAR, Inc., Houston, Texas) was used with the GPS receiver to achieve real-time 20-cm accuracy. The RMS errors for rectifying the images using first-order transformation were approximately 2 m. All images were resampled to 1 m resolution using the nearest neighborhood technique. All procedures for image registration and rectification were performed using ERDAS Imagine (ERDAS Inc., Norcross, Georgia).

Image Classification

The rectified four-band multispectral images were classified into 2-10 spectral classes using ISODATA (Iterative Self-Organizing Data Analysis) unsupervised classification (Campbell, 2002; ERDAS, 2002). The unsupervised method uses minimum spectral distance to group each pixel to a class. The process began with arbitrary class means from the image statistics based on the number of classes specified. It repeatedly performed a classification and recalculated new class statistics, which were used for the next iteration. The process continued until the number of iterations reached 200 or the convergence threshold reached 1.00. In all the classifications, the convergence threshold was met before the maximum number of iterations was reached. The spectral classes in each classification map were then grouped into root rot-infested and non-infested zones by comparing with the original image and based on ground observations. The root rot-infested areas and non-infested areas were estimated from the best two-zone classification maps.

Yang et al. (2005 and 2010) performed accuracy assessments on unsupervised classification maps derived from both multispectral and hyperspectral imagery for four different cotton fields. Their results indicate that overall accuracy of the two-zone classification maps for the four fields was from 95% to 98% and the producer's and user's accuracies for the images were from 94 to 100%. Clearly, cotton root rot infestations can be accurately identified from non-infested areas if there are no other major coexisting stressors with similar symptoms to root rot. Field observations confirmed that cotton root rot was the dominant stressor and there was a minimal amount of interference from other biotic and abiotic factors in these cotton fields. Therefore, the two-zone classification maps using the unsupervised classification and regrouping procedures were accurate and reliable. Nevertheless, care was taken to ensure infested areas were correctly identified by visually comparing each classification map with its original CIR and normal color images.

Results and Discussion

Figure 1 shows CIR images acquired on the four dates for field 1 in Edroy, TX. On the CIR images, healthy plants showed a reddish-magenta tone, while infected plants had a greenish or cyanic color. The root rot areas could be easily separated from the non-infested areas on the CIR images. Excessive rainfall in the Edroy area created very favorable conditions for the development of root rot during the early part of the 2010 growing season, but the rainfall pattern and associated cloudy weather made it difficult to take timely and complete images for the study fields. Due to sufficient moisture, it was not necessary to irrigate the field, which had two center pivots. Although all the fields were confirmed to have the onset of cotton root rot on 2 June, the first set of images was not captured until 12 July. By this date, the cotton root rot had expanded substantially within each field. The July 30 image revealed

that root continued to expand from the infected areas shown on the 12 July image. In field 1, the fungus seemed to expand predominantly in circular patterns, though some infected areas had irregular shapes. Moreover, the fungus might have either expanded outward from the center of an infected area or spread inward from the outside perimeter of an infected area towards the center. By August 11, the lower portion of the field was defoliated to prepare for harvest. There had been no significant increase in root rot from the previous date. By August 23, the field was already harvested and root rot-infested areas can be clearly seen in the image. The only difference was that most of the infested areas were taken over by weeds. That is why these areas had a reddish color on the CIR image.

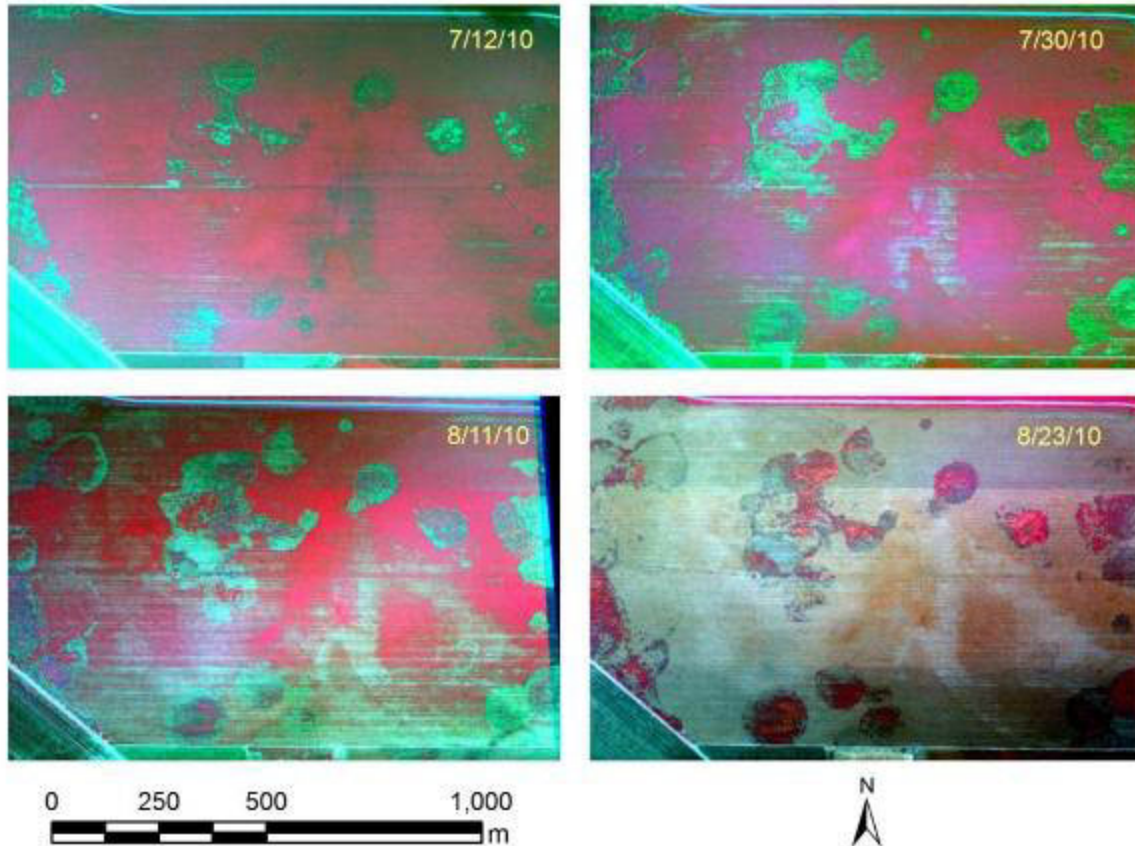


Figure 1. Airborne CIR images acquired on four dates during the 2010 growing season from a 92.5-ha cotton field (field 1) infected with cotton root rot in Edroy, TX.

Table 2 gives the percent root rot areas estimated based on the 2- to 12-class unsupervised classification maps for the 12 and 30 July dates for the two fields in Edroy. Visual evaluations of the 2- to 12-class unsupervised classification maps generated from each image revealed that the 4-class maps for both dates produced the greatest degree of separation between root rot-infested areas and non-infested areas for field 1, while the 6-class map for 12 July and the 7-class map for 30 July had the best separation for field 2.

Table 2. Percent root rot areas (%) for field 1 (92.5 ha) and field 2 (86.1 ha) in Edroy, TX on two dates during the 2010 growing season. The percent areas were estimated from 2- to 12-class unsupervised classification maps for each image.

Field	Date	Number of spectral classes										
		2	3	4	5	6	7	8	9	10	11	12
1	7/12/10	35.6	19.7	5.6	5.4	4.9	5.9	5.7	5.4	7.2	6.8	6.0
	7/30/10	19.8	14.9	13.6	11.0	10.6	14.7	15.7	17.5	14.1	14.1	13.4
2	7/12/10	33.3	15.6	12.9	12.1	17.2	16.5	18.3	23.4	21.6	24.6	18.6
	7/30/10	27.7	19.1	16.4	23.5	20.8	21.6	18.3	23.9	20.9	24.3	23.0

Figures 2 and 3 show the best unsupervised classification maps along with the respective merged 2-zone maps on the two dates for fields 1 and 2, respectively. On the multi-class unsupervised classification maps, magenta, red dark red color represent root rot areas, while the blue, cyan, green and yellow represent the areas that were not infected with root rot, but had different levels of growth variability. On the merged 2-zone classification maps, the red color represents root rot-infested areas, while the green color depicts non-infested areas. A visual comparison of the classification maps and their respective CIR images indicated that the 2-zone classification maps effectively identify apparent root rot areas within the fields. The estimated percent root rot areas in field 1 increased from 5.6% on 12 July to 13.6% on 30 July based on the 4-class classifications on both dates. In comparison, the estimated percent root rot areas in field 2 increased from 17.2% on 12 July based on the 6-class classification to 21.6% on 30 July based on the 7-class classification. In fact, the increase in field 2 was not very obvious as shown by the CIR images.

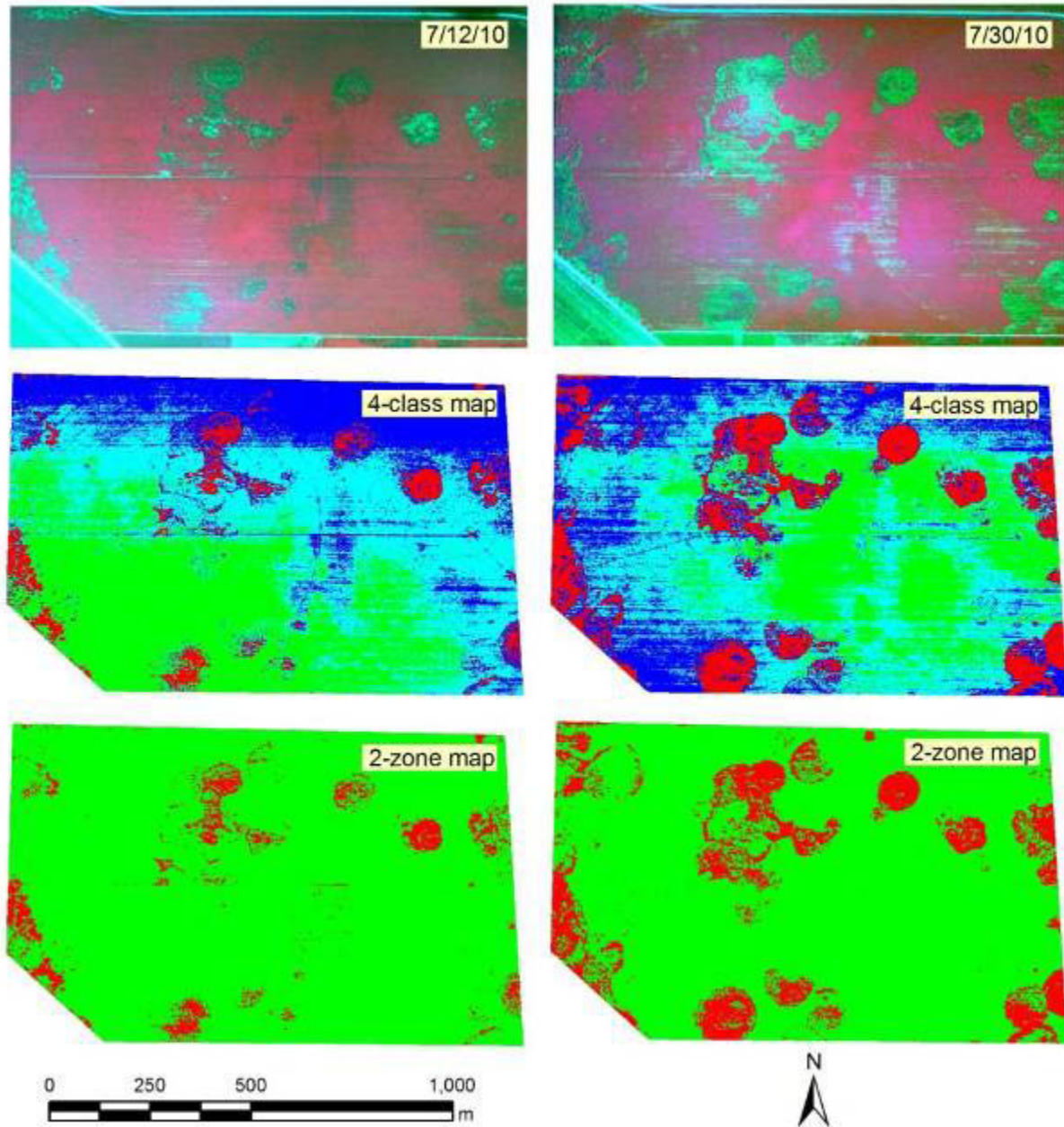


Figure 2. CIR images, 4-class unsupervised classification maps and merged 2-zone classification maps for the 12 and 30 July dates for field 1 a 92.5-ha cotton field (field 1) infected with cotton root rot in Edroy, TX. In the two-zone maps, red represents root rot-infested areas and green depicts non-infested areas.

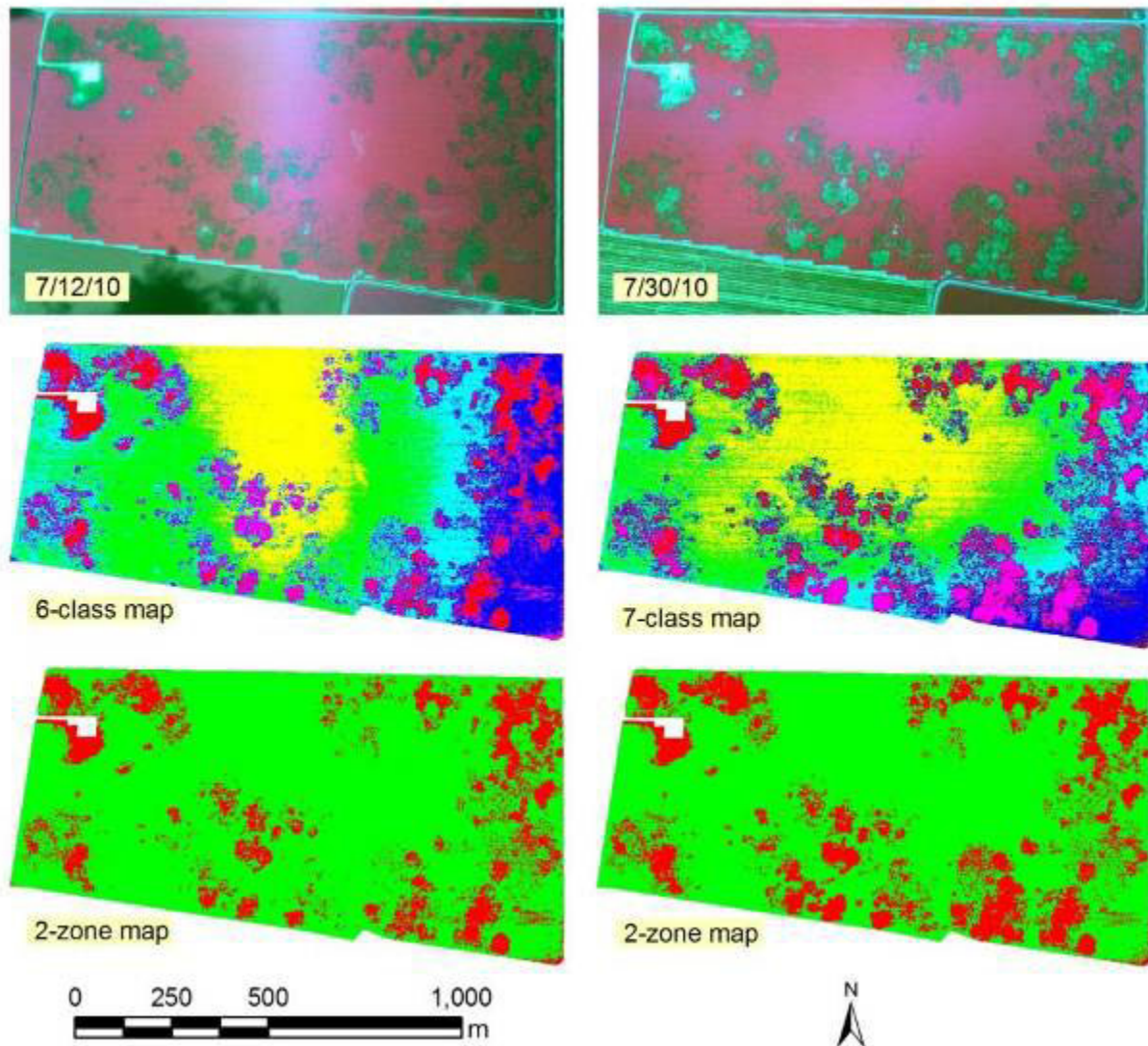


Figure 3. CIR images, 6-class unsupervised classification map for 12 July and 7-class unsupervised classification map for 30 July, and merged 2-zone classification maps for the two dates for an 86.1-ha cotton field (field 2) infected with cotton root rot in Edroy, TX. In the two-zone maps, red represents root rot-infested areas and green depicts non-infested areas.

The top portions of Figures 4 and 5 show CIR images acquired on the three dates for fields 1 and 2, respectively, in San Angelo, TX. By July 25, root rot symptoms were noted in both fields. By August 23, the fungus had spread across the fields. Unlike in field 1 in Edroy where the fungus spread dominantly in circular patterns, the fungus expanded in irregular patterns. By September 27, shortly before harvest, root rot had expanded to cover much of the fields.

Table 3 gives the percent root rot areas estimated based on the 2- to 12-class unsupervised classification maps for the 23 August and 27 September dates for the two fields in San Angelo. Visual evaluations of the 2- to 12-class unsupervised classification maps generated from each image indicated that the 6-class map for 23 August and the 4-class map for 27 September produced the best separation between root rot-infested areas and non-infested areas for field 1, whereas the 4-class map for 23 August and the 7-class map for 27 September provided the best distinction for field 2.

Table 3. Percent root rot areas (%) for field 1 (92.5 ha) and field 2 (86.1 ha) in San Angelo, TX on two dates during the 2010 growing season. The percent areas were estimated from 2- to 12-class unsupervised classification maps for each image.

Field	Date	Number of spectral classes										
		2	3	4	5	6	7	8	9	10	11	12
1	8/23/10	32.5	24.3	34.5	29.6	25.9	21.7	26.0	23.1	20.5	19.8	23.7
	9/27/10	38.6	34.8	40.4	37.8	41.9	39.0	39.9	39.9	41.2	39.5	37.8
2	8/23/10	40.6	22.3	16.9	12.9	12.6	16.5	23.0	23.8	21.0	18.6	16.6
	9/27/10	55.0	42.1	54.6	56.8	50.8	52.3	51.3	48.1	52.8	49.3	53.0

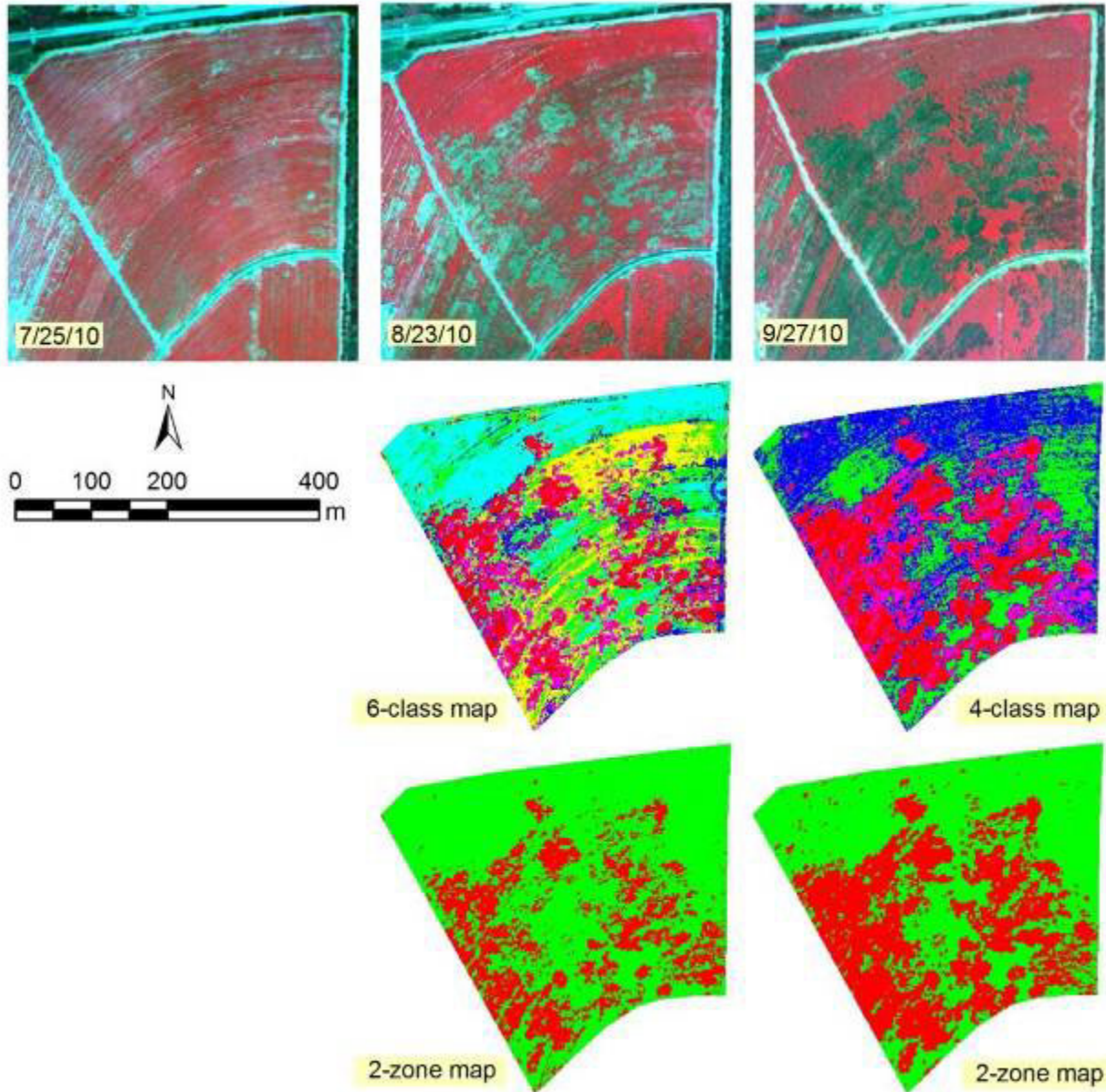


Figure 4. CIR images, 6-class unsupervised classification map for 23 August and 4-class unsupervised classification map for 27 September, and merged 2-zone classification maps for the two dates for an 11.3-ha cotton field (field 1) infected with cotton root rot in San Angelo, TX. In the two-zone maps, red represents root rot-infested areas and green depicts non-infested areas.

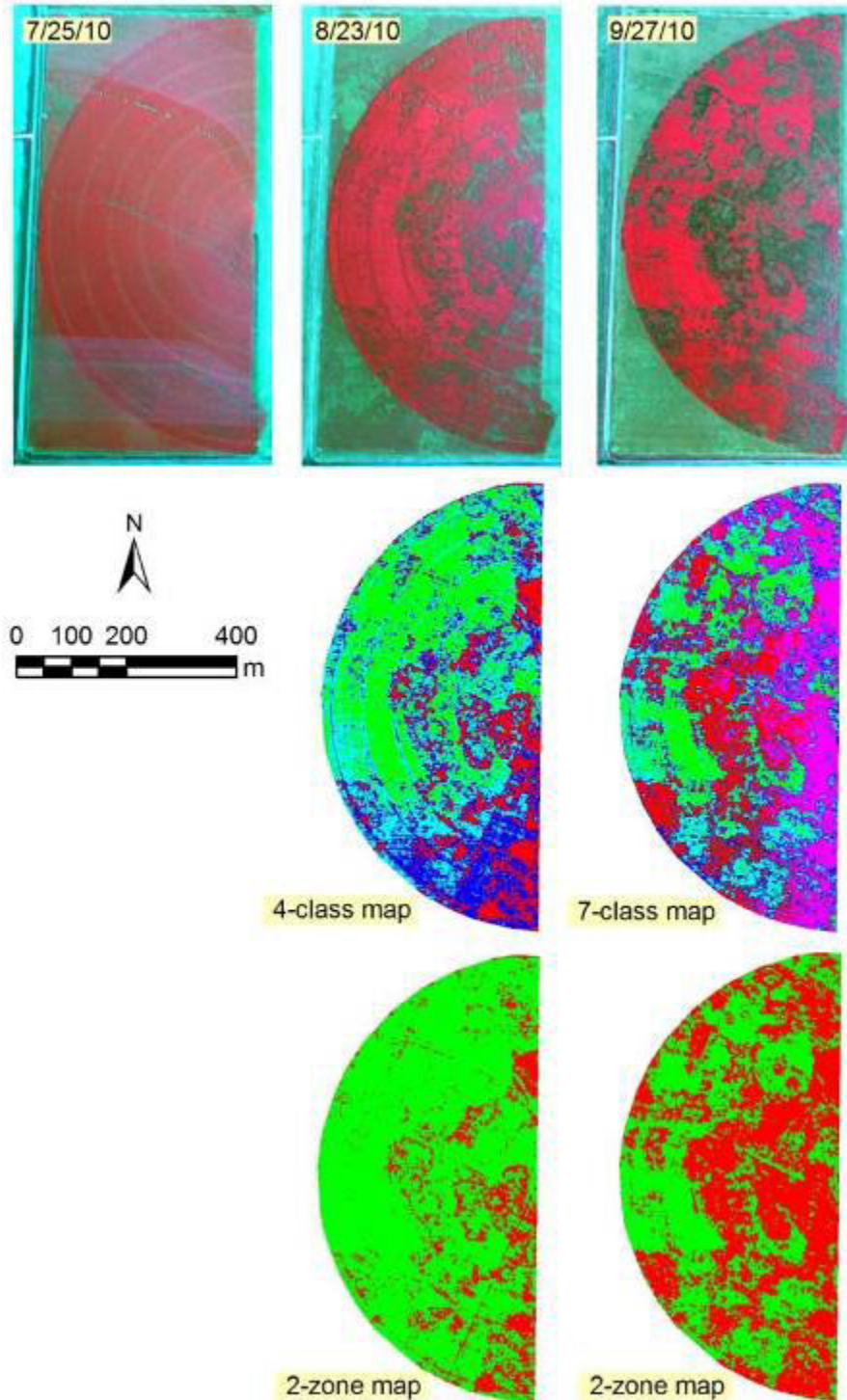


Figure 5. CIR images, 4-class unsupervised classification map for 23 August and 7-class unsupervised classification map for 27 September, and merged 2-zone classification maps for the two dates for a 25.5-ha cotton field (field 2) infected with cotton root rot in San Angelo, TX. In the two-zone maps, red represents root rot-infested areas and green depicts non-infested areas.

The middle and lower portions of Figures 4 and 5 show the best unsupervised classification maps along with the respective merged 2-zone maps on the 23 August and 27 September dates for fields 1 and 2, respectively. A visual comparison of the classification maps and their respective CIR images indicated that the 2-zone classification maps accurately identified root rot areas within the fields. The estimated percent root rot areas in field 1 increased from 25.9% on 23 August based on the 6-class classification to 40.4% on 27 September based on the 4-class classification. The estimated percent root rot areas in field 2 more than tripled from 16.9% on 23 August based on the 4-class classification to 52.3% on 27 September based on the 7-class classification.

Summary

The results from this study demonstrate that airborne multispectral imagery in conjunction with unsupervised classification is an effective tool for monitoring and mapping cotton root rot infestations within cotton fields during the growing season. Both airborne imagery and ground observations showed that cotton root rot expanded in different patterns and at different rates when compared among fields over the season. These results will be useful for the understanding of the progression of the disease and for the development of site-specific treatment plans for the disease. It should be noted that root rot was the dominant stressor in the study fields at both locations, even though other minor biotic and abiotic stressors may have been present. However, because the fungus kills cotton plants so quickly, it has a very unique signature on the airborne imagery compared with other stressors such as nutrient deficiencies and minor insect damage. Therefore, these other factors had minimal effects on the correct identification of root rot areas within the fields. Stressors that could cause plant wilting or death, as root rot did, would affect the accuracy of the root rot mapping results.

Weather was the main limiting factor for obtaining timely imagery in the 2010 growing season, especially in the Edroy area. The first set of imagery was acquired about six weeks after the initial incidence of cotton root rot was observed within the fields in Edroy. Images taken from this period would provide important information on the initiation and progression of the fungus in the early stages of its development. Nevertheless, multiple temporal images were obtained from each field to monitor the progression and document the extent of the fungus towards the end of the growing season. The images and classification maps from this study will be useful for studies of the interactions among soil properties and other biological, crop growth, and environmental factors associated with cotton root rot. For long-term effective and economical management of this disease, it is necessary to not only understand the within-season expansion patterns, but also to monitor the consistency and variation of the spatial patterns from year to year. Therefore, more research is needed to study the consistency and variation in initiation time, expansion rate and infestation extent of this disease over multiple years using remote sensing and other emerging technologies in a multidisciplinary approach.

Acknowledgements

This project was partly funded by Cotton Incorporated, Cary, NC. The authors wish to thank Michael Ohlinger of Sterling Air Service at Weslaco, TX and Fred Gomez of USDA-ARS at Weslaco, TX for taking the multispectral imagery for this study and Jim Forward of USDA-ARS at Weslaco, TX for assistance in image processing.

References

- Campbell, J.B. 2002. Introduction to Remote Sensing, 3rd ed. The Guilford Press, NY.
- ERDAS. 2002. ERDAS Field Guide. ERDAS Inc., Norcross, GA.
- Ezekiel, W.N. and J.J. Taubenhaus. 1934. Cotton crop losses from *Phymatotrichum* root rot. J. Agric. Res. 49(9):843-858.
- Fernandez, C.J., C. Yang, and J.H. Everitt, 2005. Late-planting decreased cotton root rot infestations in irrigated fields. Proceedings of Beltwide Cotton Conferences, National Cotton Council of America, Memphis, Tennessee, pp. 197-202.
- Isakeit, T., R.R. Minzenmayer, J. Stapper, and C.G. Sansone. 2007. Evaluation of fungicides for control of cotton root rot caused by *Phymatotrichopsis omnivora*. Proceedings of Beltwide Cotton Prod. Res. Conf., pp. 181-184.

- Isakeit, T., R.R. Minzenmayer, and C.G. Sansone. 2009. Flutriafol control of cotton root rot caused by *Phymatotrichopsis omnivora*. Proceedings of Beltwide Cotton Conferences, pp. 130-133.
- Lyda, S.D., and E. Burnett. 1970. Influence of benzimidazole fungicides on *Phymatotrichum omnivorum* and *Phymatotrichum* root rot of cotton. *Phytopathology* 60:726-728.
- Lyda, S.D., G.D. Robison, and H.W. Lembright. 1967. Soil fumigation control of phymatotrichum root rot in Nevada. *Plant Disease Reporter* 51(5):331-333.
- Nixon, P.R., S.D. Lyda, M.D. Heilman, and R.L. Bowen. 1975. Incidence and control of cotton root rot observed with color infrared photography. Pub. No. MP1241. Texas A&M Agricultural Experiment Station, College Station, TX.
- Nixon, P.R., D.E. Escobar, and R.L. Bowen. 1987. A multispectral false-color video imaging system for remote sensing applications. Proceedings of 11th Biennial Workshop on Color Aerial Photography and Videography in the Plant Sciences and Related Fields, 295-305, 340. American Society for Photogrammetry and Remote Sensing, Bethesda, MD.
- Olsen, M.W. 2009. Cotton (Texas) Root Rot. Pub. No. AZ1150. The University of Arizona Cooperative Extension, Tucson, AZ.
- Rush, C.M. and T.J. Gerik. 1989. Relationship between postharvest management of grain sorghum and *Phymatotrichum* root rot in the subsequent cotton crop. *Plant Disease* 73(4):304-305.
- Rush, C.M., and S.D. Lyda. 1984. Evaluation of deep-chiseled anhydrous ammonia as a control for phymatotrichum root rot of cotton. *Plant Disease* 68:291-293.
- Smith, H.E., F.C. Elliot, and L.S. Bird. 1962. Root rot losses of cotton can be reduced. Pub. No. MP361. Texas A&M Agricultural Extension Service, College Station, TX.
- Taubenhaus, J.J., W.N. Ezekiel, and C.B. Neblette. 1929. Airplane photography in the study of cotton root rot. *Phytopathology* 19:1025-1029.
- Whitson, R.S., and R.B. Hine. 1986. Activity of propiconazole and other sterol-inhibiting fungicides against *Phymatotrichum omnivorum*. *Plant Disease* 70:130-133.
- Yang, C. 2010. A high resolution airborne four-camera imaging system for agricultural applications. ASABE Paper No. 1008856, American Society of Agricultural and Biological Engineers, St. Joseph, Michigan.
- Yang, C., C.J. Fernandez, and J.H. Everitt. 2005. Mapping *Phymatotrichum* root rot of cotton using airborne three-band digital imagery. *Transactions of the ASAE* 48(4):1619-1626.
- Yang, C., C.J. Fernandez, and J.H. Everitt. 2010. Comparison of airborne multispectral and hyperspectral imagery for mapping cotton root rot. *Biosystems Engineering* 107:131-139.